

Fig.1: ROC curves for in-mean and in-variance causality.

Purpose. Granger Causality (GC) approaches have recently been employed to estimate the directionality of the influence exerted by a brain region on another. Despite the fact that fluctuations in the BOLD signal at rest contain important information about the physiological processes that underlie neurovascular coupling, so far associations between brain signals have focused on central tendencies (i.e. mean or median) and have modeled this compounded variability as noise. A possible causative structure in the variability of brain activity remains completely unexplored.

Methods and materials. In this contribution, we develop a theoretical framework for simultaneous estimation of both in-mean and in-variance causality in complex networks. We validate our approach in synthetically-generated signals from complex networks of coupled nonlinear Kuramoto oscillators and employ it on fMRI Human Connectome Project (HCP) data in order to estimate of in-variance connectome of the human brain.

Results. Fig. 1 shows ROC curves obtained for both in-mean and in-variance causal network reconstruction in synthetic validation. Applying the framework to *in vivo* data, structured and distinct in-mean and in-variance causal connectomes emerge. Fig. 2 shows circular plots highlighting the top 1% connections belonging to the matrices derived from HCP data.

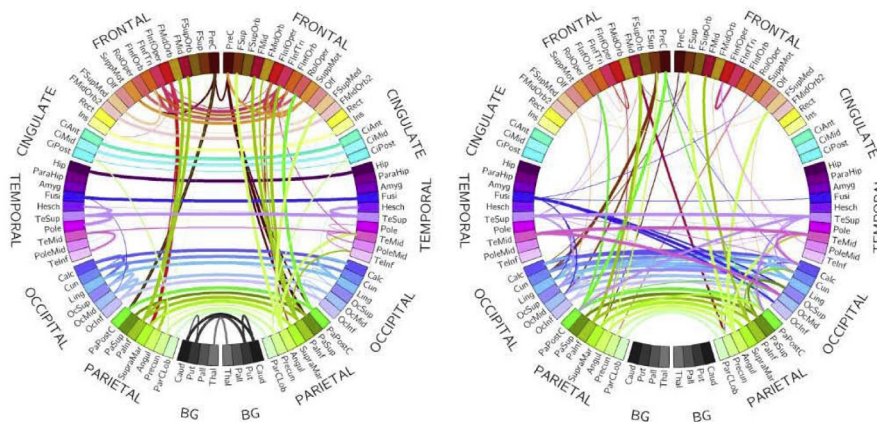


Fig.2: overall median for 100 unrelated subjects. Every edge (i.e. connection) is colored according to the node (i.e. anatomical ROI) which is driving the other node.

Conclusion. Our results serve as proof of principle for demonstrating the relevance of targeted experimental investigation about the origin of coupled fluctuations in variance in BOLD signals measured using fMRI.

<https://doi.org/10.1016/j.ejmp.2018.04.262>

252. Prediction of subject-specific SAR distribution in MSK MR exam at 7 T

V. Gagliardi^a, G. Tiberi^{a,b}, L. Biagi^a, A. Retico^c, M.R. Symms^d, R. Stara^e, G. Aringhieri^f, V. Zampa^f, M. Tosetti^{a,b}

^aIRCCS Stella Maris, Pisa, Italy

^bIMAGO7, Pisa, Italy

^cINFN, Pisa Section, Pisa, Italy

^dGeneral Electric ASL Scientist (EMEA), Pisa, Italy

^eStanford University, Stanford, CA, USA

^fDiagnostic and Interventional Radiology, University of Pisa, Pisa, Italy

Purpose. we predict SAR during MRI exam using a 7 T ¹H 298 MHz eight-channel degenerate birdcage coil¹ combining SAR simulations with subject-specific measured (RF) B_1^+ maps.

Materials and Methods. We simulated the coil¹ in CST MW Suite, loaded by a model of human knee (Fig. 1, top). B_1^+ was calculated in an axial slice crossing the patella. The maximum local SAR for an Axial “Zero” Time-of-Echo (ZTE) sequence “SILENT”² was calculated.

We acquired $|B_{1,map}^+|$ maps of an adult (female) knee with a Bloch-Siegert sequence on 7 axial slices, centered on the same slice of the simulation, on a GE MR950 7T human system. For each slice a coefficient C, proportional to $\text{avg}(|B_{1,map}^+|)/B_{1,nominal}^+$, was used to scale the SAR simulated³.

Results. Fig. 1 shows: bottom left, simulated B_1^+ magnitude; bottom center, local SAR for an input of 1 W per channel; bottom right, simulated $B_{1,nominal}^+$ magnitude for a FA = 90° (length = 3.2 ms) sinc-pulse in the slice previously chosen.

Fig. 2 shows the subject-specific measured $|B_{1,map}^+|$ for a FA = 90° sinc-pulse. The predicted SAR obtained with scaled B_1^+ maps are 0.50 W/kg (global) and 3.68 W/kg (maximum).

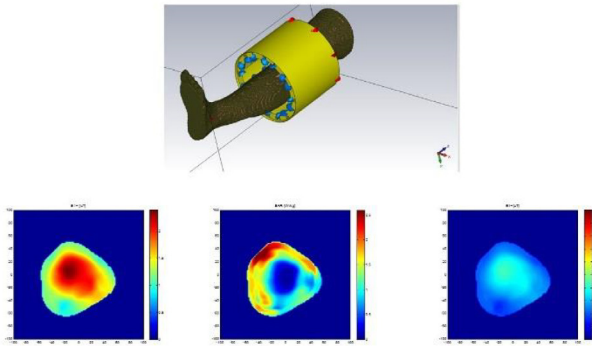


Fig. 1

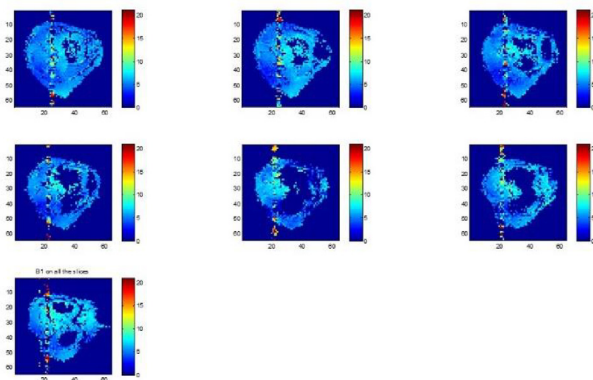


Fig. 2

Conclusions. we obtained a good agreement between simulated and measured *in vivo* B_1^+ maps, and we were able to calculate the distribution of SAR exposure, a safety MRI parameter not available in current exams, where only global SAR is provided, combining simulations and subject-specific measurements. Limits on global and local SAR (20 W/kg) were met for this sequence [1–3].

References

1. Stara R. A Degenerate Birdcage with Integrated Tx/Rx Switches and Butler Matrix for the Human Limbs at 7 T, *Appl Magn Reson* 2017;48(3):307–26.
2. Costagli M. Assessment of SILENT T1-weighted head imaging at 7 Tesla, *Eur Radiol* 2016;26(6):1879–88.
3. Tiberi G. SAR prediction in Adults and Children by combining measured B_1^+ maps and simulations at 7.0 T. *JMRI* 2016;44(4):1048–55.

<https://doi.org/10.1016/j.ejmp.2018.04.263>

253. An accurate and operator independent method for biological tumour volume segmentation

Giorgio Russo^{a,c}, Albert Comelli^{a,b,e}, Alessandro Stefano^a, Maria Gabriella Sabini^c, Massimo Ippolito^d, Maria Carla Gilardi^a, Anthony Yezzi^e

^aInstitute of Molecular Bioimaging and Physiology, National Research Council (IBFM-CNR), Cefalù (PA), Italy

^bDepartment of Industrial and Digital Innovation (DIID), University of Palermo (PA), Italy

^cMedical Physics Unit, Cannizzaro Hospital, Catania, Italy

^dNuclear Medicine Department, Cannizzaro Hospital, Catania, Italy

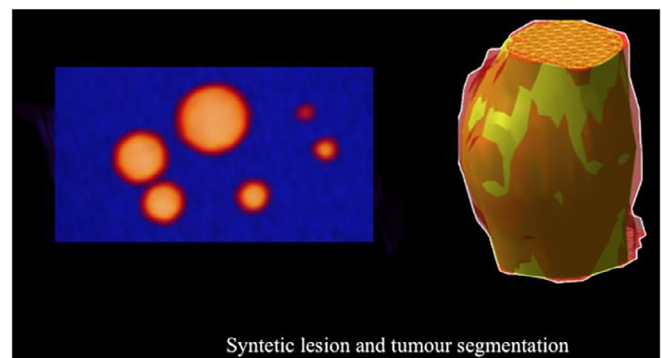
^eDepartment of Electrical and Computer Engineering, Georgia Institute of Technology, Atlanta, USA

Purpose. The aim of this paper is to develop an operator independent method for biological tumour volume (BTV) delineation from Positron Emission Tomography (PET) images. BTV delineation is challenging because of the low spatial resolution and high noise level in PET images. In addition, BTV varies substantially depending on the method used to segment. Manual delineation is widely-used, but it is strongly user dependent.

Methods. The proposed method starts with the automatic identification of the PET slice with maximum Standardized Uptake Value (SUV). Then, a user-independent mask is obtained by a rough pre-segmentation step and it is used to perform the local active contour segmentation on the next slices. When the proposed method finds a slice where the mean SUV on the interior of the delineation contour is greater or equal than the mean SUV on the exterior of the delineation contour, the segmentation is automatically stopped. The algorithm is evaluated on four datasets of synthetic lesions considering different ratios between lesion and background radioactivity concentrations. In this way, the actual lesion volumes are known and the segmentation algorithm is evaluated under different contrast ratio scenarios. In addition, BTVs of 25 patient studies have been manually delineated and compared to the proposed method in order to assess its applicability in a clinical environment.

Results. In phantom experiments, dice similarity coefficient (DSC) rate and true positive volume fraction (TPVF) rate greater than 90% were observed in synthetic lesions with a diameter greater than 17 mm. In clinical cases, TPVF and DSC were $91.00 \pm 7.33\%$ and $85.98 \pm 3.40\%$, respectively.

Conclusion. Our method produces accurate segmentation results in phantom studies. In addition, it is feasible in clinical context and shows good accuracy in realistic conditions, reducing any user interaction.



<https://doi.org/10.1016/j.ejmp.2018.04.264>

254. Fast T1,T2, M0 mapping in clinical MRI: Look-locker based inversion recovery balanced turbo field echo

P.R. Dicarolo^a, A. Ciccarone^a, C. Defilippi^a, G. Zatelli^b

^aMeyer Children's University Hospital, Radiology Department, Florence, Italy

^bUSL Toscana centro p.zza Santa Maria Nuova 1, Florence, Italy